Misorientations of garnet aggregate within a vein: an example from the Sanbagawa metamorphic belt, Japan

Submitted to JMG

Misorientations of garnet aggregate within a vein: an example from the Sanbagawa metamorphic belt, Japan

(Misorientations of garnet aggregates)

A. OKAMOTO[1], K. MICHIBAYASHI[2]

[1] *Institute of geosciences, Shizuoka University, Shizuoka 422-8529, Japan*

Present address: *Graduate School of Environmental Studies, Tohoku University, Sendai, 980-8579, Japan*

[2] *Institute of geosciences, Shizuoka University, Shizuoka 422-8529, Japan*

ABSTRACT

In this study, the chemistry and microstructure of garnet aggregates within a metamorphic vein are investigated. Garnet-bearing veins occur subparallel to the foliation of a host mafic schist in the Sanbagawa metamorphic belt, Japan. Backscattered electron image and compositional mapping using EPMA and crystallographic orientation maps from electron-backscattered diffraction (EBSD) reveal that numerous small garnet (10-100 m diameter) coalesces to form large porphyroblasts within the vein. Individual small garnet commonly exhibits xenomorphic shape at garnet/garnet grain boundaries, whereas idiomorphic at garnet/quartz boundaries.

EBSD microstructural analysis of the garnet porphyroblasts reveals that misorientation angles of neighbour-pair garnet grains within the vein have a random distribution. This contrasts with previous studies that found coalescence of garnet in mica schist leads to an increased frequency of low angle misorientation boundaries by misorientation-driven rotation. As garnet nucleated with random orientation, the difference in misorientation between the two studies is due to the difference in the

extent of grain rotation. A simple kinetic model that assumes grain rotation of garnet is rate-limited by grain boundary diffusion creep of matrix quartz shows that (1) the substantial rotation of a fine garnet grain could occur for the conditions of the Sanbagawa metamorphism, but (2) the rotation rate drastically decreased as garnet grains formed large clusters during growth. Therefore, the random misorientation distribution of garnet porphyroblasts in the Sanbagawa vein is interpreted as follows: (1) garnet within the vein grew so fast that substantial grain rotation did not occur through porphyroblast formation, and thus (2) random orientations at the nucleation stage were preserved. The extent of misorientation-driven rotation indicated by deviation from random orientation distribution may be useful to constrain the growth rate of constituent grains of porphyroblast that formed by multiple nucleation and coalescense.

Keyword: garnet aggregate, misorientation, coalescence, grain rotation, vein

INTRODUCTION

Misorientation magnitudes between mineral grains in metamorphic rocks provide us significant information on histories of deformation and growth of mineral aggregates (e.g., Wheeler *et al.*, 2001, Skemer *et al.*, 2005). In the studies of metals and ceramics, it has been documented that grain boundaries with small misorientations have low interfacial energies (e.g., Gleiter, 1982; Sutton & Baluffi, 1987; Chan & Baluffi, 1995; Saylor & Rohrer, 1999), and that grain rotation acts to reduce interfacial energy (Sutton & Baluffi, 1987; Chan & Baluffi, 1995). Recently, Spiess *et al*. (2001) analyzed garnet porphyroblasts in mica schist from the Eastern Alps, and proposed a porphyroblast growth model that consists of multiple nucleation, coalescence and misorientation-driven grain rotation. Using a simple kinetic model, Spiess *et al*. (2001) showed that substantial rotation of garnet grains of a size <100 m is possible during regional metamorphism. Although their work showed that misorientation analyses are applicable to investigate microstructural development during mineral growth, few natural examples of this grain-rotation process have been reported.

In this study, we investigate the microstructure of garnet porphyroblasts, that

is composed of numerous fine grains, within a metamorphic vein in a mafic schist from the Sanbagawa metamorphic belt, Japan. The garnet porphyroblasts analyzed in this study have several similarities to that studied by Spiess *et al*. (2001), indicating that they also formed by multiple nucleation and coalescense. However, there is an important difference in the misorientation angle distribution. Based on the detailed microstructural observations and a simple kinetic model of Spiess *et al.* (2001), we discuss what controls the progressive grain rotation of mineral aggregates during the formation of porphyroblasts.

GEOLOGICAL SETTING

The Sanbagawa metamorphic belt is a high-pressure intermediate type metamorphic belt that extends 700-800 km along the Japanese islands (Miyashiro, 1961). The Sanbagawa schists are mainly composed of pelitic, mafic and quartz schist with minor psammitic schists. The Sanbagawa belt is divided into four mineral zones on the basis of index minerals within pelitic schists of increasing metamorphic grade: chlorite zone, garnet zone, albite-biotite zone and oligoclase-biotite zone (Higashino 1990; Fig. 1). The

dominant structural features of Sanbagawa metamorphic rocks include a gently north-dipping foliation and a subhorizontal east-west mineral lineation. The mineral lineation is generally considered to have formed during or after the peak metamorphism (Wallis 1990; 1998). In central Shikoku, the highest-grade oligoclase-biotite zone is located in the middle of the structural sequence, and the metamorphic grade decreases both northwards and southwards. This pattern is considered to represent a large south-vergent recumbent fold formed during exhumation of the Sanbagawa belt (Banno & Sakai, 1989).

The analyzed sample was collected from the albite-biotite zone in the Besshi area, central Shikoku (Fig. 1). The peak metamorphic temperature of this area was estimated to be 520±25˚C by the garnet-chlorite geothermometer, 530±60˚C by the garnet-biotite geothermometer, and 500-550 ˚C by the calcite-dolomite geothermometer (Enami *et al.*, 1994). The peak pressure was estimated to be 8-9.5 kbar from the equilibria of sodic pyroxene- bearing assemblage (Enami *et al.*, 1994).

ANALYTICAL METHODS

The microstructure and chemistry of garnet within a garnet-bearing vein were investigated from thin sections cut perpendicular to the foliation and parallel to the lineation of the host mafic schist. Orientation contrast (OC) images were taken by a field-emission gun SEM (JEOL JSM6500) in the Center for the Advanced Marine Core Research, Kochi University. The chemical compositions of minerals were analyzed using an electron-probe microanalyser (EPMA; JEOL8900) at the University of Tokyo, operated at an acceleration voltage of 15 kV, and beam current of 12 nA for quantitative analyses and 120 nA for map analyses. The number of cations per formula unit of garnet was calculated based on the assumption of O = 12, and Fe^{3+} was calculated as $2 - Al^{3+}$. X_{Al} is defined as $Al / (Al + Fe^{3+})$. Mole fractions of pyrope (X_{prp}), almandine (X_{alm}), grossular (X_{grs}) and spessartine (X_{sps}) are calculated as $X_{prp} = Mg/(Mg + Fe^{2+} + Ca + Mn) \times X_{Al}$. Crystallographic preferred orientations (CPO) and misorientation magnitudes of garnet were measured by indexation of Electron Back-Scattered Diffraction (EBSD) using a JEOL JSM6300 system at Shizuoka University. EBSD patterns were indexed using CHANNEL+ software from HKL Technology (Schmidt & Olesen, 1989).

OCCURRENCE OF GARNET-BEARING VEIN

The Sanbagawa schist contains a variety of mono- and polymineralic veins filled with quartz, calcite, chlorite, albite, epidote, muscovite and actinolite. Angles between the vein walls and the foliation plane are predominantly high (>60˚), but continuously change from 90˚ to 0˚ (Toriumi & Hara, 1995; Toriumi & Yamaguchi, 2000). Toriumi & Hara (1995) demonstrated that low-angle veins have formed earlier than high-angle veins based on the fact that (1) high-angle cracks cut low-angle veins and (2) quartz in low-angle veins contain abundant subgrains due to deformation. The veins intersecting the foliation at high-angles are interpreted to have developed during the late stage exhumation of the Sanbagawa belt.

The garnet-bearing veins occur within a large body of albite-biotite zone mafic schist in the Besshi area (Fig. 1). The mafic schist is composed of amphibole, epidote, albite, chlorite, quartz, titanite, rutile, phengitic mica, and calcite. Prominent foliation and lineation are defined by the alignment of amphibole, epidote, chlorite and mica. Amphibole shows a clear compositional zoning of barroisite → hornblende →

actinolite from core to rim. This zoning pattern indicates that amphibole grew during the exhumation of the Sanbagawa belt (Otsuki & Banno, 1990; Okamoto & Toriumi, 2004; 2005). Garnet-bearing veins appear as brownish layers or lenses of 0.1 - 30 cm thick (Fig. 2a and b). They occur subparallel to the foliation of the surrounding mafic schist, and some clearly cut the foliation at low angle (<30˚) (Fig. 2b). They are commonly folded in harmony with the host mafic schist (Fig. 2a).

The garnet-bearing vein analyzed in this study has a thickness of 3-5 mm (Fig. 2c) and is composed dominantly of quartz and garnet with small amounts of pyrite, ilmenite, amphibole, chlorite, epidote, and apatite. According to the modal abundance of minerals, we subdivide the vein into two parts: garnet-dominant and quartz-dominant parts (Fig. 2c). In the garnet-dominant part, fine-grained garnets comprise 60 vol.% and cluster-forming large aggregates. Amphibole, chlorite, pyrite and ilmenite are also abundant in the garnet-rich part. The quartz-rich part consists of >80 vol. % quartz, and garnets commonly occur as isolated grains. The boundary between the two parts is subparallel to the vein wall. The mafic schist adjacent to the vein contains a ~3 mm alternation zone characterized by the presence of garnet, pyrite and ilmenite in addition

to the mineral assemblage of the host mafic schist.

Quartz grains are commonly elongate subparallel to the layer boundary, and have an aspect ratio of 1 – 4 (Fig. 2d). Quartz commonly exhibits undulose extinction, and grain boundaries are restricted by the presence of garnet and amphibole grains. Quartz is coarse-grained in the quartz-dominant part (~80 m in diameter), and much finer in the garnet-dominant part (~ 50 m in diameter). Amphibole and epidote within the garnet-rich layer have a columnar habit, and are aligned parallel to the layer boundary. Amphibole has compositional zoning of barroisite → hornblende → actinolite from core to rim. This zoning pattern is also observed in amphibole of the host rock. Pyrite is commonly mantled by ilmenite (Fig. 2e). Within the vein, ilmenite also includes garnet. Chlorite formed along garnet/garnet boundaries with thickness of < 2 m, and commonly replaces garnet.

CHARACTERISTICS OF VEIN GARNET

Microstructures

Within the garnet-bearing vein, garnet occurs as isolated grains or as an aggregate of

fine grains. Isolated garnet crystals within a quartz matrix are commonly idiomorphic, except for minor irregularities and rounded outlines (Fig. 3a). These isolated garnets are 10-100 m in diameter.

Garnets commonly impinge upon each other, especially in the garnet-rich part of the vein, and commonly form large porphyroblasts composed of aggregates of fine grains (Fig. 2c). The detailed microstructure of porphyroblasts cannot be observed using an optical microscope, but BSE and orientation contrast (OC) images show grain boundaries between fine garnet grains (Fig. 3b, c, d, e). Electron-backscattered diffraction (EBSD) analysis reveals that most of these boundaries are grain boundaries, and not subgrain boundaries. The largest observed porphyroblast is ~2.0 mm in diameter, and is composed of more than one thousand garnet grains. The size of the constituent garnet grains varies systematically from the center to the margin of the porphyroblast. Here, we use the terms "center" and "margin" for positions within a porphyroblast, and "core" and "rim" for positions within individual grains following the terminology of Spiess *et al.* (2001). Garnet grains are smallest within the center of porphyroblasts (5-10 m in diameter), and are larger toward the margin (50-100 m in

diameter; Fig. 3c, d, e). This trend of grain size within porphyroblasts is not concentric, but is recognized mainly in direction normal to the foliation. Within the center of the porphyroblasts, the garnet aggregate has a mosaic-like structure (Fig. 3e), and grains range from idiomorphic to xenomorphic. Fractures commonly develop within large porphyroblasts in direction subnormal to the vein wall (Fig. 3c and e).

Compositional zoning and growth microstructure

Garnet within the vein shows a clear chemical zoning from core to rim. Figure 4 shows X-ray maps of Mn zoning, and Fig. 5 shows compositional profiles from core to rim. Representative compositions of garnet are listed in Table 1. Analyzed garnets are rich in almandine ($0.54 < X_{alm} < 0.62$) and grossular ($0.29 < X_{grs} < 0.35$) components.

Porphyroblast 1 is composed of 11 grains (G1-G11), and each grain displays clear compositional zoning (Fig.4a, Fig. 5a). X_{prp} increases steadily from core to rim, while X_{alm} has a maximum concentration within the interior of the grains. X_{grs} has peak concentrations within the core and within the interior of the grains. X_{sps} has two peaks within the interior of the grain. X_{Al} (= Al / (Al + Fe^{3+})) gradually increases toward the

rim from 0.92 to 1.0. This indicates that Fe^{3+} was contained in the octahedral site of garnet during the early stages of growth. To identify the growth microstructure, we subdivided each garnet grain into four regions (region 1 - 4) on the basis of Mn zoning (Fig. 4a). Some grains in Porphyroblast 1 do not have regions 1 and 2, probably because these grains were not cut through their core. Regions 1 and 2 show a concentric growth surface of idiomorphic garnet. In contrast, outlines of regions 3 and 4 show irregular shapes at their boundaries where impingement against adjacent grains has occurred. Consequently, the growth surfaces of regions 3 and 4 are far from concentric. At the growth stage of region 4, garnet overgrew on the surface contact with quartz or amphibole, whereas the growth ceased at the garnet/garnet boundary. Along some garnet/garnet boundaries, quartz and chlorite are precipitated with the width of < 10 m (G1/G7, G1/G2, G4/G7 and G2/G8 boundaries). At such boundaries, the outlines of garnet grains on both sides are in harmony with each other. Thus, these boundary microstructures were formed by fracturing after the porphyroblast formation.

Porphyroblast 2 is a large garnet aggregate composed of numerous fine garnets (Fig. 3d, Fig. 4b). Each fine garnet grain has a clear compositional zoning

similar to that of Porphyroblast 1 (region 1 - 4). Garnet grains are larger in the porphyroblast margin than those in the center (Fig. 3e). The small grains in the center have concentric growth surfaces of region 1 and 2, but show irregular shape of region 3 and 4 due to restriction by adjacent garnet grains (Fig. 4b'). The large grains in the porphyroblast margin show a highly asymmetric growth pattern. They grew predominantly at outer sites of the porphyroblast (Fig. 4b).

The zoning pattern of garnet in the host mafic schist is different from that of garnet within the vein (Fig. 4c, Fig. 5c). Fe^{2+} and Mg contents monotonously increase, and Ca and Mn contents decrease (Fig. 5c). Fe^{3+} content in this garnet is very low (<0.02). The compositional zoning of garnet in the mafic schist is comparable to that in region 4 of garnet in the garnet-bearing vein (Fig. 5a, c).

Crystallographic preferred orientation and misorientation

Figure 6a shows a band contrast image of Porphyroblast 2 from EBSD crystallographic orientation mapping. Crystallographic orientations of garnets were well indexed, and the colored lines in Fig. 6a indicate grain boundaries with angle of 2-10˚, 10-20˚, 20-30˚

and >30˚. The outlines of individual garnet grains in the EBSD map are consistent with those recognized by BSE imaging and EPMA compositional mapping (Fig. 3d, e, Fig. 4b).

The CPO pattern of isolated garnet grains within the garnet-bearing vein is shown in Fig. 6b. The CPO pattern is very weak. The CPO patterns of garnets were also measured for several porphyroblasts within the vein. For every porphyroblast, the CPO pattern is very weak, and we did not find any meanings from the pattern (Fig. 6c).

Misorientation angles and misorientation axes for individual boundaries in Porphyroblast 1 are listed in Table 2. Among 11 grains, most boundaries have misorientations in the range 40 – 60 ˚, and misorientation angle < 10˚ is only found at the G3 / G4 boundary. No systematic trends are apparent in the misorientation axes data. Within the larger porphyroblast (porphyroblast 2), low angle boundaries are rare and most boundaries show misorientations of >30˚ (Fig. 6a). Distributions of random-pair and neighbour-pair misorientations for Porphyroblast 2 were derived from orientation maps. For this porphyroblast, both distributions are completely consistent with the theoretical curve of the random orientation of garnet (Grimmer, 1980) (Fig. 6d). No

systematic changes of misorientation magnitudes were observed with respect to the grain size or location within the porphyroblast.

DISCUSSION

Timing of the formation of the garnet-bearing vein

It is difficult to estimate the P-T conditions of garnet crystallization within the vein, due to the lack of an activity model for garnet that includes Fe^{3+} component. It is also unclear as to whether garnet grew in equilibrium with other vein minerals. However, we consider that the garnet-bearing veins formed at close to peak metamorphic temperatures (500 - 550 ˚C) during Sanbagawa metamorphism, based on the following points:

1) The garnet-bearing veins occur subparallel to the foliation, and are folded in harmony with the mafic schist (Fig. 2a, b and c). This indicates that the vein formed before or during foliation development within the host schist. The foliation of the mafic schist is defined by the alignment of amphibole, which is mainly composed of

barroisite and hornblende. The amphibole growth of barroisite → hornblende is thought to have occurred with decreasing pressure at high temperatures (> ~500 ˚C) (Okamoto & Toriumi, 2005).

2) Chemical zonation within the rims of garnet (region 4; Fig. 4a, Fig. 5a) from the vein and that of garnet from adjacent alternation zone (Fig. 4c, Fig. 5c) is characterized by bell-shaped Mn zoning and a monotonous increase in Mg. Bell-shaped Mn growth zoning is generally considered to represent an increase of temperature (e.g., Banno *et al*., 1986; Enami, 1998; Inui & Toriumi, 2002).

3) Mafic schist was pervasively affected by retrograde reactions under greenschist facies conditions. An important retrograde reaction involved hydration to produce actinolite and chlorite (Okamoto & Toriumi, 2005). If the vein was associated with this reaction, the reaction progress should vary with distance from the vein. No systematic changes of the modal abundance of actinolite and chlorite across the vein are recorded, and this indicates that the garnet-bearing veins were formed prior to the greenschist facies overprint.

Origin of garnet porphyroblasts within the vein: comparison with garnet aggregates described in previous studies

The recent development of EBSD has enabled the investigation of garnet crystallographic orientation, and it has been demonstrated that garnet CPO and low-angle misorientation boundaries can develop via dislocation creep and the coalescense of multiple garnet crystals (e.g., Prior *et al.*, 2000; Kleinschrodt & MacGrew, 2000; Spiess *et al.,* 2001; Kleinschrodt & Duyster, 2002; Prior *et al.,* 2002; Ji *et al.,* 2003; Mainprice *et al.,* 2004; Storey & Prior, 2005; Terry & Heidelbach, 2004; Wheeler *et al.,* 2001).

One possible mechanism of forming a large porphyroblast with internal subdomains is the breakdown of a single garnet porphyroblast via plastic deformation. Prior *et al.* (2002) investigated a deformed garnet from an upper-amphibolite facies shear zone within eclogite of the Glenelg-Attadale inlier, NW Scotland. They found that misorientation angles measured across subdomain boundaries are significantly lower than those for random pairs, and concluded that the domain boundaries are likely to be subgrain boundaries formed via dislocation creep and recovery. Storey & Prior (2005)

developed the work of Prior *et al.* (2002), and showed that garnet porphyroblasts from Glenelg record an evolution from dislocation and recovery accommodated deformation under low-strain conditions, through dynamic recrystallization by subgrain rotation, to diffusion creep assisted grain boundary sliding under high-strain conditions. Garnets analyzed in our study rarely contain subdomain boundaries with low misorientation magnitude (Fig. 6a, Table 2), and some show clear idiomorphic crystal surfaces at garnet/garnet boundaries and within the crystal interior (Fig. 4a). Thus, deformation by dislocation creep is not considered a likely mechanism to explain the porphyroblast microstructure formation within the studied vein.

A second possible mechanism of porphyroblast formation is the coalescense of multiple fine-grained garnets. Spiess *et al*. (2001) investigated the microstructure of garnet aggregates in mica schist of the Paleozoic western Schneeberg Complex in the Eastern Alps. They found that garnet porphyroblasts contain numerous fine garnets both with and without subdomains. Misorientation magnitudes between garnet subdomains in analyzed porphyroblasts deviate from a random distribution curve, and reveal an increase of the number of low angle (<20˚) misorientations. Spiess *et al*. also found

nearly random orientations for individual fine garnet grains within the porphyroblast. To explain these observations, Spiess *et al*. suggested that garnet nucleated with initial random orientations, and that coalescense and boundary misorientation-driven rotation of small garnet occurred during porphyroblast formation (Fig. 7a). Garnet porphyroblasts within the vein analyzed in this study are similar to those described by Spiess *et al.* (2001) in terms of microstructure, metamorphic conditions, matrix minerals, and size of garnet subdomains (Table 3). A common feature of the two studies is that garnet grains (subdomains) are larger in the margin of the aggregate than those in the center. In addition, individual garnet grains in our sample show a random orientation as similar to that of Spiess *et al.* (Fig. 6b). An important difference between the two studies is that garnet grains within the porphyroblasts in the vein from the Sanbagawa schist rarely have any subdomains with low misorientation magnitude (Fig. 6a, Table 3), resulting in a random distribution in misorientation (Fig. 6d).

Terry & Heidelbach (2004) investigated the microstructure of garnet corona in an eclogite-facies shear zone from Haram Gabbro, Norway. They reported a high frequency of low-angle subgrain boundaries in the weakly deformed sample and an

increase of the number of high misorientation boundaries with increasing strain. As strain increases, the CPO becomes weaker and the misorientation angle distribution approaches a random distribution. They interpreted the low-angle subgrain boundaries as resulting from the growth of similarly oriented garnet nuclei, and proposed that deformation by grain boundary sliding resulted in large misorientation boundaries. The weak CPO patterns and high frequency of large misorientation angles for garnet porphyroblasts analyzed in this study (Fig. 6c, d) is comparable to the patterns observed by Terry & Heidelbach (2004) in high strain rocks. However, the porphyroblasts within the vein are not considered to be associated with deformation by grain boundary sliding for the following reasons. (1) The compositional zonings of coalesced grains shows symmetric patterns across the boundary, and no mismatch due to the grain rotation was observed (Fig. 4a). (2) Although some garnet-bearing veins are folded (Fig. 2a), deformation of the vein was probably accommodated by plastic deformation of quartz and brittle deformation of garnet porphyroblasts. EBSD analyses show that garnet grains on both sides of a fracture have quite different crystallographic orientations (G1/G7, G1/G2, G4/G7 and G2/G8 boundaries of Porphyroblast 1; Fig. 3a, Table 2).

This indicates that fractures developed along pre-existing subdomain boundaries within garnet porphyroblasts. Within large porphyroblasts, fractures commonly developed in direction perpendicular to the foliation along the network of subdomain boundaries (Fig. 3c and e). Irregular shape of the porphyroblasts (Fig. 3d) and non-concentric subdomain size distribution within the porphyroblasts (Fig. 3d, e) may also result from later fracturing in subnormal to the foliation and pull-apart. Fractures are rare within garnet grains without subdomain and amphibole grains, indicating that fracture strength of garnet porphyroblast with subdomain was much lower than other brittle minerals.

In conclusion, it is considered that the random misorientation distribution of garnet porphyroblasts within the vein is a record of the multiple nucleation of garnets with random orientations. As individual garnets grew, they coalesced to form large porphyroblasts.

What controls the extent of misorientation-driven rotation?

The microstructural features of garnet porphyroblasts analyzed in this study are indicative of multiple-nucleation with random orientation and coalescense, as described

above (Table 3). However, the misorientation distribution in our sample is a contrast to that of Spiess *et al.* (2001). In the sample of Spiess *et al.* (2001), the misorientation angle with highest frequency is lower than that of random orientation distribution by 40-50˚ (Figs. 9 and 18 of Spiess *et al.*, 2001), whereas the misorientation distribution of our sample is very close to a random distribution (Fig. 6c). This indicates that substantial grain rotation and associated reduction in interfacial energy is not necessarily a corollary of porphyroblast formation via coalescense.

As garnet nucleated with random orientation in both cases (Table 3), the difference in the misorientation distribution is due to difference in the extent of rotation of garnet grains. The misorientation distribution of Spiess *et al.* (2001) indicates that many grains within the porphyroblasts rotated at least 40˚ (Figs. 9 and 18 of Spiess *et al.*, 2001). On the other hand, the result of our sample implies a very small extent of the rotation. Considering the uncertainties of the misorientation analyses (~2˚) and the resolution of the histogram (5˚), the rotation was probably less than 5˚ (Fig. 6c).

One possible factor to produce the difference in the extent of grain rotation is the rotation rate of garnet. Spiess *et al*. (2001) presented a simple kinetic model

describing coalescence and misorientation-driven rotation of fine garnet grains (Fig. 8a). Their model assumes that (1) the rotation of garnet grains was impeded by the surrounding quartz matrix, and consequently (2) the rotation rate of garnet grains ($d\theta/dt$) is comparable to the strain rate within the quartz matrix (de/dt), and (3) quartz deformed by pressure solution / coble creep. The diffusivity of grain boundary diffusion of Si at temperature T is expressed as $D_{GB} = D_{0GB}exp(-H_{GB}/RT)$, where H_{GB}, and R are the activation energy for grain boundary diffusion, and the gas constant respectively. Following the model of Spiess *et al*. (2001), the rotation rate of a garnet grain, $d\theta/dt$, for the geometry shown in Fig. 8a is described as follows:

$$d\theta/dt = de/dt = A\Omega\psi r\pi\delta D_{0GB}exp(-H_{GB}/RT)/kTw^2d^3, \quad (1)$$

where A, Ω, δ and k are a constant, atomic volume, grain boundary width and Boltzmann constant, respectively. ψ indicates the loss in surface energy per unit area as misorientation is reduced by 1 radian. The derivation of equation 1 is detailed in Spiess *et al*. (2001).

The times taken for a garnet grain to rotate by 1˚ were calculated from equation 1 for the conditions of this study (dashed curve) and of Spiess *et al.* (2001) (solid curve), respectively (Fig. 8b). The values of parameters used in equation 1 are as determined by Spiess *et al*. (2001; Table 4). The temperature of formation of garnet porphyroblast was set to be 550˚C for this study (Table 3). Calculations were carried out to obtain the rotation rates of garnet grains with 10, 20, 30, 50, 100 and 500 m diameter. As described in Spiess *et al.* (2001), the rotation rate increases with increasing size of garnet/garnet (subdomain) boundaries (*2r*) and with decreasing grain size of rotating garnet (*w*). In the garnet-rich part of the analyzed vein, 10 - 20 m garnets are common in the center of a porphyroblast, and the quartz grain size is ~50 m. For such a case, the time taken to rotate 1˚ is estimated to be 10^3-10^4 years (shaded circle in Fig. 8b). Results shown in Fig. 8b and similar subdomain size of garnet (<100 m) between two studies show that the rotation rate for the condition of the Sanbagawa vein is close to that of Spiess *et al.* (2001), and suggest that the rate is large enough to produce substantial rotation. Therefore, the rotation rate as estimated above cannot explain the substantial difference in misorientation distribution between the two studies.

A most-likely factor to explain the variation in misorientation distribution is growth rate of garnet. Without growth, a single garnet grain coalescing in the adjacent grain will keep rotating at constant rate as long as it exists at high-temperature. However, as garnet grows after the coalescense (increase of grain size of rotating garnet, *w*), the rotation rate will decrease (Fig. 6b). Furthermore, for the case that many garnets form a large aggregate during growth, Spiess *et al*. (2001) discussed that clustering leads to an increase in the size of initially fine-grained garnets, which in turn leads to a reduction in the rate of crystal rotation. Following the formation of an aggregate, garnet grains are resistant to further rotation. Accordingly, the grain rotation becomes negligible small after the formation of a large porphyroblast (> 500 m; Fig. 6b). In addition, if individual coalesced garnets grow rapidly relative to the misorientation-driven rotation, they will develop xenomorphic grain boundaries with precipitation in the spaces initially filled by quartz (Fig. 7b). Such xenomorphic concavo-convex boundaries at garnet/garnet boundaries were clearly observed in the porphyroblasts (G1/G3, G3/G5, G8/G9 boundaries in Fig. 4a, Fig. 4b'). Therefore, the rapid growth relative to grain rotation of garnet prevented the further rotation, which would result in

the preservation of the primary random orientation of garnets.

Implication

Spiess *et al*. (2001) discussed that the estimated rotation rate (several thousand to several tens thousand years for 1˚ rotation) indicates the possibility of substantial rotation of garnet during regional metamorphism over several million years. In contrast, random orientation of garnets within the porphyroblast in our sample indicates that the duration was not enough for substantial rotation of garnet. Assuming grain rotation was less than 5˚, the order of the estimated timescale (10^3-10^4 years for 1˚ rotation) may comparable to the upper-limit of the duration of garnet rotation. This duration is quite brief compared with the 10^7-10^8 years duration of the Sanbagawa metamorphism (Itaya & Takasugi, 1988). Since the misorientation angle distribution would have been frozen after the porphyroblast formation, the estimated timescale for garnet rotation is comparable to the duration of garnet crystallization (porphyroblast formation) within the vein.

It is noted that the model of Spiess *et al.* (2001) assumes that garnet is

surrounded by quartz at growth stage. The uncommon Fe^{3+}-rich composition (Fig. 3a and b, Table 1) and the occurrence in association with pyrite of garnet analyzed in this study imply that garnet grew in association with influx of external fluid. Therefore, it is expected that garnet was partly in contact with fluid as well as quartz. As aqueous fluid is much less resistant to garnet rotation than quartz, garnet would have rotated faster than as estimated from equation 1.

Porphyroblast formation by multiple nucleation and coalescense could occur in rocks that initially had an extremely high density of garnet nuclei. However, such a high population density of garnet is not commonly observed in the Sanbagawa schist. In the case of this study, multiple nucleation of garnet would have resulted from the deviation from equilibrium conditions due to influx of external fluid. In common pelitic and mafic schists in the Sanbagawa belt, garnet is coarser-grained (50 - 1000 m), and the number of grains per unit area is much smaller. Accordingly, the coalescense of garnet grains is rare, and coalesced grains, if present, do not have low misorientation angles due to their large grain size. Garnets within pelitic schist in the albite-biotite zone of the Sanbagawa schist are commonly ~300 m in radius, and record a prograde *P-T*

path from 470˚C, 0.6 GPa to 520 ˚C, 0.9 GPa as determined from compositional zoning (Inui & Toriumi, 2002). This indicates that garnets grew during the subduction of the slab from 18 km to 27 km in depth. If we assume a convergence rate at the plate boundary of 1-5 cm / year and a subduction angle of 30˚, the duration of garnet growth is then $3.6 \times 10^4 - 1.8 \times 10^5$ year. As a consequence, the average growth rate of garnet with radius of 300 m in pelitic schist is $10^{-4} - 10^{-2}$ m / year. In contrast, assuming the duration of garnet growth within the vein to be $< 10^3$ years, the lower-limit of growth rate of garnet with radius of 100 m is 10^{-1} m / year. Garnet may have grown in the vein at least $10 - 10^3$ times faster than garnet growth within the pelitic schist.

CONCLUDING REMARKS

As previously acknowledged by Spiess *et al.* (2001), the model of misorientation-driven rotation is very simple, and the values of some of the parameter used in the calculation have large uncertainties. However, the similarities in microstructure and metamorphic conditions between our study and that of Spiess *et al.* (2001) indicate a similar origin of

the studied garnet aggregates. In addition, the contrasting misorientation distribution patterns indicate a significant difference in the growth rate of garnet within the vein compared with garnet within the host rock. It's possible to interpret that the growth rate of minerals within the vein is much greater than for minerals in the host rock.

Metamorphic mineral growth is accompanied by the development of microstructures such as grain shape, CPO and misorientations. As for the porphyroblast formation by multiple-nucleation and coalescense, the extent of grain rotation, which would change in response to growth rate as well as temperature, may be recorded in the misorientation distribution pattern. Recently, Skemer *et al.* (2005) has suggested a quantitative indicator of misorientation distribution pattern (misorientation index) showing the deviation from random orientation distribution. Application of such a indicator and development of a grain rotation model for the evolution of misorientation distribution will allow us to understand the growth kinetics of mineral aggregates more in detail.

ACKNOWLEDGEMENTS

We would like to thank T. Masuda and H. Yamaguchi for discussions and encouragements, and A. Stallard for improving the early version of the manuscript. We thank H. Yoshida for help with EPMA analyses at the University of Tokyo. Thanks are due to D. Prior and R. Spiess for extensive review, and to D. Robinson for editorial handling. This study is financially supported in part by JSPS Research Fellowship for Young Scientists to A. Okamoto.

REFERENCES

Banno, S., Sakai, C. & Higashino, T., 1986. Pressure-temperature trajectory of the Sanbagawa metamorphism deduced from garnet zoning. *Lithos*, **19**, 51-63.

Banno, S., & Sakai, C., 1989. Geology and metamorphic evolution of the Sanbagawa metamorphic belt, Japan. In *Evolution of Metamorphic Belts* (eds Daly, J.S., Cliff, R.A., Yardley, B.W.D.), **43**, PP. 519-532, Geological Society, London, Special Publication.

Chan, S. & Baluffi, R. W., 1995. Study of energy vs misorientation for grain boundaries in gold by crystallite rotation method – I. [001] twist boundaries. *Acta Metallurgica*, **6**,

1113-1119.

Enami, M., Wallis, S. R. & Banno, Y., 1994. Paragenesis of sodic pyroxene-bearing quartz schists: implication for the P-T history of the Sanbagawa belt. *Contributions to Mineralogy and Petrology*, **116**, 182-198.

Enami, M., 1998. Pressure-temperature path of Sanbagawa prograde metamorphism deduced from grossular zoning of garnet. *Journal of Metamorphic Geology*, **16**, 97-106.

Gleiter, H., 1982. On the structure of grain boundaries in metals. *Materials Science and Engineering*, **52**, 91-131.

Grimmer, H., 1980. A unique description of the relative orientation of neighbouring grains. *Acta Crystallographica*, **24**, 353-359.

Higashino, T., 1990. The higher-grade metamorphic zonation of the Sanbagawa metamorphic belt, in central Shikoku Japan. *Journal of Metamorphic Geology*, **8**, *413-423.*

Inui, M. & Toriumi, M., 2002. Prograde pressure-temperature paths in the pelitic schists of the Sambagawa metamorphic belt, SW Japan. *Journal of Metamorphic Geology*, **20**,

563-580.

Itaya, T. & Takasugi, H., 1988. Muscovite K-Ar ages of the Sanbagawa schists, Japan and argon depletion during cooling and deformation. *Contributions to Mineralogy and Petrology*, **100**, 281-290.

Ji, S., Saruwatari, K., Mainprice, D., Wirth, R., Xu, Z. & Xia, B. 2003. Microstructures, petrofabrics and seismic properties of ultra high-pressure eclogites from Sulu region, China: implications for rheology of subducted continental crust and origin of mantle reflections. *Tectonophysics,* **370**, 49-76.

Kleinschrodt, R. & McGrew, A., 2000. Garnet plasticity in the lower continental crust: implication for deformation mechanisms based on microstructures and SEM-electron channeling pattern analysis. *Journal of Structural Geology*, **22**, 795-809.

Kleinschrodt, R. & Duyster, J. P., 2002. HT-deformation of garnet: an EBSD study on granulites from Sri Lanka, India and the Ivrea Zone. *Journal Structural Geology*, **24**, 1829-1844.

Mainprice, D., Bascou, J., Cordier, P. & Tommasi A., 2004. Crystal preferred orientations of garnet: comparison between numerical simulations and electron back-

scattered diffraction (EBSD) measurements in naturally deformed eclogites. *Journal of Structural Geology*, **26**, 2089-2102.

Miyashiro, A., 1961. Evolution of metamorphic belts. *Journal of Petrology*, **2**, 277-311.

Okamoto A. & Toriumi, M., 2004. Optimal mixing properties of calcic and subcalcic amphibole solid solution: application of Gibbs' method to the Sanbagawa schists, SW Japan. *Contributions to Mineralogy and Petrology*, **146**, 529-545.

Okamoto, A. & Toriumi, M. 2005. Progress of actinolite-forming reaction during retrograde metamorphism: an example from mafic schists in the Sanbagawa belt, Japan. *Journal of Metamorphic Geology,* **23**, 335-356.

Otsuki, M. & Banno, S., 1990. Prograde and retrograde metamorphism of hematite-bearing mafic schists in the Sanbagawa belt in central Shikoku. *Journal of Metamorphic Geology*, **8**, 425-439.

Prior, D.J., Wheeler, J., Brenker, F.E., Harte, B. & Matthews, M., 2000. Crystal plasticity of natural garnet: New microstructural evidence. *Geology*, **28**, 1003-1006.

Prior, D. J., Wheeler, J., Peruzzo, L., Spiess, R. & Storey, C., 2002. Some garnet microstructures: an illustration of the potential of orientation maps and misorientation

analyses in microstructural studies. *Journal of Structural Geology*, **24**, 999-1011.

Saylor, D. M & Rohrer, G. S., 1999. Measuring the influence of grain boundary misorientation groove geometry in ceramic polycrystals. *Journal of the American Ceramic Society*, **82**, 1536.

Schmidt, N. H. & Olesen N. O., 1989. Computer-aided determination of crystal lattice orientation from electron channeling patterns in the SEM. *Canadian Mineralogist*, **27**, 15-22.

Skemer, P., Katayama, I., Jiang, Z. & Karato, S. 2005. The misorientation index: Development of a new method for calculating the strength of lattice-preferred orientation. *Tectonophysics*, **411**, 157-167.

Spiess, R., Peruzzo, L., Prior, D. J. & Wheeler, J. 2001. Development of garnet porphyroblasts by multiple nucleation, coalescence and boundary misorientation-driven rotations. *Journal of Metamorphic Geology*, **19**, 269-290.

Storey, C. D. & Prior, D. J. 2005. Plastic deformation and recrystallization of garnet: A mechanism to facilitate diffusion creep. *Journal of Petrology*, **46**, 2593-2613.

Sutton, A. P. & Baluffi, R. W., 1987. On geometric criteria for low interfacial energy.

Acta Metallurgica, **35**, 2177-2201.

Terry, M. P. & Heidelbach, F. 2004. Superplasticity in garnet from eclogite facies shear zones in the Haram Gabbro, Harasøya, Norway. *Geology*, **32**, 281-284.

Toriumi, M. & Hara, E., 1995. Crack geometries and deformation by the crack-seal mechanism in the Sambagawa metamorphic belt. *Tectonophysics*, **245**, 249-261.

Toriumi, M. & Yamaguchi, H., 2000. Dehydration and the mechanics of metamorphic belts. *Journal of Geography*, **109**, 600-613 (in Japanese with English abstract).

Wallis, S., 1990. Timing of folding and stretching in the Sanbagawa belt, the Asemigawa region, central Shikoku. *Journal of Geological Society of Japan*, **96**, 345-352.

Wallis, S., 1998. Exhuming the Sanbagawa metamorphic belt: the importance of tectonic discontinuities. *Journal of Metamorphic Geology*, **16**, 83-95.

Wheeler, J., Prior, D. J., Jiang, Z., Spiess, R., & Trimby, P. W., 2001. The petrological significance of misorientations between grains. *Contributions to Mineralogy and Petrology*, **141**, 109-124.

Figure captions

Fig. 1 Metamorphic zonation within the Sanbagawa belt, central Shikoku, Japan (Higashino, 1990). M. T. L. indicates Median tectonic line. Sample locality is marked by a star.

Fig. 2 (a), (b) Outcrop photographs of garnet-bearing veins within mafic schist. The foliation of the mafic schist is shown by while broken line. (a) Garnet-bearing veins are often folded in harmony with the host mafic schist. (b) Some garnet-bearing veins clearly cut the foliation of the host mafic schists at low angle. (c) Photomicrograph of the garnet-bearing vein analyzed in this study under plane polarised light. (d) Photomicrograph of the vein for the region indicated by the left open square in (c). (e) Back-scatter electron image of pyrite mantled by ilmenite within the vein. Grt = garnet, Am = amphibole, Qtz = quartz, Ep = epidote, Pyt = pyrite, Ilm = ilmenite.

Fig. 3 (a) BSE image of an isolated garnet crystal within a quartz matrix in the sampled vein. (b) OC image of a garnet porphyroblast (Porphyroblast 1) composed of several

coalesced crystals. (c) BSE image of garnet porphyroblasts composed of numerous fine grains for the right open square shown in Fig. 2b. (d), (e) BSE images of garnet porphyroblast composed of numerous fine grains (Porphyroblast 2). The darker grey parts within garnet in BSE images correspond to higher Mn rim of garnets. Arrows in Fig. 2c and e indicate fractures within garnet porphyroblast along network of subdomain boundaries.

Fig. 4 X-ray maps of Mn concentration within garnets. Lighter gray indicates higher Mn content. Compositional profiles along A-A', B-B' and C-C' are shown in Fig. 5. (a) A garnet porphyroblast within the vein (Porphyroblast 1) and accompanying sketch. This porphyroblast is composed of 11 coalesced grains (G1-G11). Solid line indicates grain or subgrain boundaries recognized from OC image (Fig. 3b). Each garnet is divided into four regions (region 1 – 4) on the basis of Mn zoning patterns. (b) A garnet porphyroblast composed of numerous fine garnets (Porphyroblast 2). The close-up image indicates that garnets within Porphyroblast 2 have similar compositional zoning to those within Porphyroblast 1. (c) Garnet within the host rock.

Fig. 5 Line profile of garnet composition. X_{Al} indicates Al / (Al+Fe^{3+}) along (a) A-A' in Fig. 4a, (b) B-B' in Fig. 4b and (c) C-C' in Fig. 4c.

Fig. 6 Electron Back-Scattered Diffraction (EBSD) data for garnet within the vein shown in Fig. 4b. (a) A band contrast image with grain boundaries (2-10˚, 10-20˚, 20-30˚, >30˚) of Porphyroblast 2. Mapping is carried out by 2.5 mm step, and grid of 300×400. Region coloured by white outside the porphyroblast represents minerals other than garnet. (b), (c) Poles to {100}, {111}, and {110} planes for (b) isolated garnet grains and (c) garnet grains within Porphyroblast 2. Equal area projection, lower hemisphere. Contours are in multiples of uniform distribution. Foliation is vertical (XY plane; solid line) and lineation of the host rock is horizontal within the plane of the foliation. (d) Misorientation magnitude frequency of neighbour-pair and random-pair garnet crystals of the Porphyroblast 2 derived from the orientation map (Fig. 6a). The cutoff angle due to measurement is 2˚. The line shows the misorientation magnitude frequency for a random orientation distribution (Grimmer, 1980; Moroviec, 1995).

Fig. 7 Schematic models that illustrate garnet porphyroblast formation by multiple nucleation and coalescense in quartz matrix. Idiomorphic garnet growth surface is shown by a hexagon shape, and crystallographic orientation is shown by white arrow. In both cases, garnet initially has random orientation ($t = t_0$), and growth rate of garnet is negligible small at garnet/garnet boundaries. (a) Garnets grew slowly and impinged at $t = t_{1,a}$. Some coalesced garnet grains rotated to reduce interfacial energy, which lowers the misorientation angle (Spiess *et al.*, 2001). Rotation ceases following the formation of the garnet porphyroblast. More detail of this model is shown in fig. 22 in Spiess *et al.* 2001. (b) Garnets grew rapidly and impinged at $t = t_{1,b}$. Rapid overgrowth of garnet fixes the orientation of each grain, and a random orientation of garnets at $t = t_0$ is preserved during porphyroblast formation.

Fig. 8 (a) Outline of the kinetic model reproduced from fig. 21c of Spiess *et al.* (2001). A rotating grain is represented by a cylinder of diameter *w* and height h. The radius of the subdomain boundary (*r*) is smaller than that of rotating grain (*w*/2). The rotational

torque is calculated from the energy change associated with a reduction of misorientation, and the torque is converted to the shear stress for the geometry of Fig. 8a. The shear stress causes grain boundary diffusion creep in the surrounding quartz matrix, and this controls the rate of garnet rotation.

(b) Rate of garnet rotation. The figure shows the number of years taken for a garnet grain to rotate 1˚ with respect to the diameter of the garnet/garnet (subdomain) boundary (2*r*), as calculated from the kinetic model of Spiess *et al.* (2001). *w* and *d* indicates the diameter of rotating garnet grains and quartz grain size, respectively. Solid and dashed curves indicate conditions of Spiess *et al.* (2001) (T = 600 ˚C, *d* = 100 m) and this study (T = 550˚C, d = 50 m), respectively. For each curve, time taken for the rotation has a minimum when the size of subdomain boundary is equal to that of rotating grain. A shaded circle indicates the region for 10 - 20 m garnet and 50 m quartz, that corresponds to the case of garnet-rich part of the vein.

Table 1. Chemical compositions of garnet within the vein shown in Fig. 4a.

	core	→	→	Mn peak1	→	→	→	Mn peak2	→	rim
		region1		region2		region3		region4		
SiO_2	37.57	37.91	37.37	37.66	37.71	37.97	38.13	38.41	38.63	38.79
TiO_2	0.07	0.00	0.01	0.02	0.02	0.02	0.16	0.17	0.14	0.11
Al_2O_3	20.10	19.75	19.78	19.96	20.32	20.23	21.08	21.30	21.35	21.51
FeO	26.99	26.75	26.98	26.94	28.09	29.78	27.65	26.40	26.13	25.89
MnO	2.90	3.73	4.11	4.41	3.34	1.44	2.13	3.72	3.24	3.45
MgO	0.26	0.25	0.30	0.29	0.32	0.32	0.84	0.95	1.10	1.36
CaO	12.03	11.82	11.24	10.45	10.25	10.24	10.43	10.32	10.31	10.25
Na_2O	0.01	0.00	0.01	0.03	0.00	0.00	0.05	0.02	0.00	0.01
K_2O	0.00	0.00	0.01	0.01	0.00	0.00	0.00	0.00	0.00	0.00
Cr_2O_3	0.00	0.00	0.00	0.00	0.00	0.01	0.02	0.00	0.00	0.00
Total	99.94	100.21	99.79	99.76	100.04	100.00	100.49	101.29	100.89	101.36
Cation (O = 12)										
Si	3.019	3.041	3.014	3.041	3.034	3.057	3.041	3.036	3.058	3.051
Ti	0.004	0.000	0.001	0.001	0.001	0.001	0.009	0.010	0.008	0.006
Al	1.904	1.867	1.880	1.899	1.926	1.919	1.981	1.984	1.992	1.994
Fe^{3+}	0.096	0.133	0.120	0.101	0.074	0.081	0.019	0.016	0.008	0.006
Fe^{2+}	1.717	1.661	1.699	1.718	1.816	1.924	1.825	1.729	1.722	1.696
Mn	0.198	0.253	0.281	0.302	0.228	0.098	0.144	0.249	0.217	0.230
Mg	0.031	0.029	0.036	0.035	0.039	0.038	0.099	0.112	0.129	0.159
Ca	1.036	1.015	0.971	0.904	0.884	0.883	0.891	0.874	0.874	0.864
Na	0.002	0.000	0.001	0.004	0.000	0.000	0.008	0.003	0.000	0.001
K	0.000	0.000	0.001	0.001	0.000	0.000	0.000	0.000	0.000	0.000
$Al/(Al + Fe^{3+})$	0.952	0.933	0.940	0.950	0.963	0.960	0.991	0.992	0.996	0.997
X_{alm}	0.576	0.561	0.569	0.581	0.612	0.654	0.617	0.583	0.585	0.575
X_{prp}	0.010	0.010	0.012	0.012	0.013	0.013	0.034	0.038	0.044	0.054
X_{grs}	0.347	0.343	0.325	0.305	0.298	0.300	0.301	0.295	0.297	0.293
X_{sps}	0.066	0.086	0.094	0.102	0.077	0.033	0.049	0.084	0.074	0.078

Table 2. Misorientation angles and axes between grains (G1-G11) in Porphyroblast 1(Fig. 4a). Angle indicates the range of six angle data per boundary.

Boundary	angle (˚)	axis
G1-G2	43.2 - 44.2	<-3-32>
G1-G3	23.2 - 24.7	<120>
G1-G4	30.0 - 31.3	<1-41>
G1-G5	44.1 - 44.8	<2-10>
G2-G7	43.2 - 43.5	<-314>
G2-G8	31.6 - 33.0	<412>
G2-G10	39.9 - 40.1	<1-20>
G3-G4	7.2 - 8.2	<03-2>
G3-G5	57.2-57.9	<01-1>
G4-G7	55.2 - 56.6	<11-1>
G5-G6	37.5 - 38.4	<4-31>
G7-G8	44.6 - 46.2	<-2-2-1>
G8-G9	52.6 - 53.6	<-321>
G8-G11	45.5 - 46.5	<430>
G8-G10	53.7 - 55.4	<143>
G10-G11	50.4 - 51.3	<3-24>

Table3. Characteristics of garnet aggregate in the vein from the Sanbagawa belt and that reported by Spiess *et al.* (2001).

	this study	Spiess *et al.* 2001
Occurrence	vein within mafic schist from the Sanbagawa belt	mica schists from the Palaeozoic Western Schneeberg Complex of the Eastern Alps
temperature	500-550˚C	600 ˚C
matrix mineral	quartz	quartz
mean quartz grain size	50 μm	100 μm
subdomain of garnet porphyroblast	present	present
shape of individual garnet grains or subdomains	some have idiomorphic shapes, whereas others are xenoblastic	some have idiomorphic shapes, whereas others are xenoblastic
size of subdomain in garnet porphyroblast	small in the center and large in the margin of the porphyrblast.	small in the center and large in the margin of the porphyrblast.
chemical zoning of garnet	present	present
CPO of garnet with subdomain	random orientation	clustering around a single orientation
misorientation across subdomain boundaries	random distribution	an increase of the number of low angle (<20˚) misorientation with respect to random orientation
CPO of individual garnet grains	random orientation	random orientation
misorientation between garnets of individual garnet grains	random distribution	random distribution

Table 4. List of variables and values used in the calculation.

Variable	Parameters	Value
θ	misorienatation	°
e	strain	
A	constant	21*
Ω	atomic volume	8.75×10^{-29} m*
ψ	loss in surface energy per unit area as misorientation reduced by 1 rad	0.001 kJm^{-2}*
δD_{0GB}	(grain boundary width) x (grain boundary diffusion coefficient)	1.6 x 10-10 m^3s^{-1}*
H_{GB}	activation energy for grain boundary diffusion	220 $kJmole^{-1}$*
r	radius of garnet-garnet boundary	(m)
w	diameter of garnet subdomain	(m)
d	grain size of quartz	(m)
T	temperature	(K)
R	gas constant	
k	Boltzmann constant	1.831×10^{-23} JK^{-1}

* Values were followed by Spiess et al. (2001).

Fig. 1

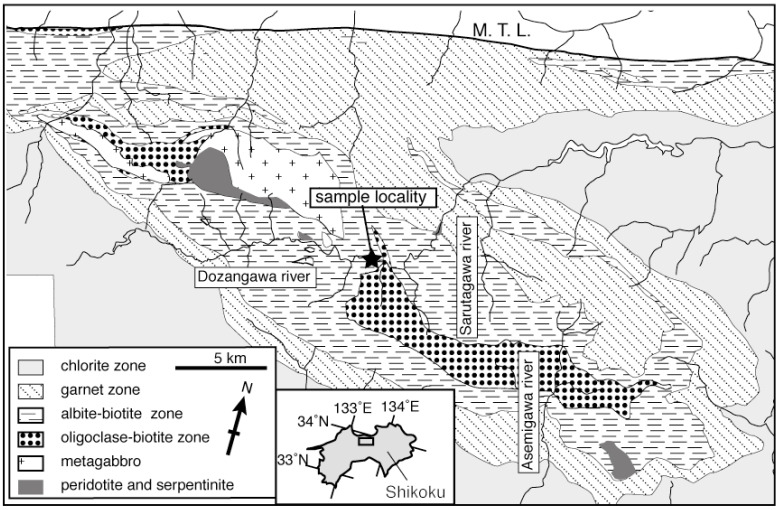
M. T. L.
sample locality
Dozangawa river
Sarutagawa river
Asemigawa river
chlorite zone
garnet zone
albite-biotite zone
oligoclase-biotite zone
metagabbro
peridotite and serpentinite
5 km
N
133°E
134°E
34°N
33°N
Shikoku

Fig. 2

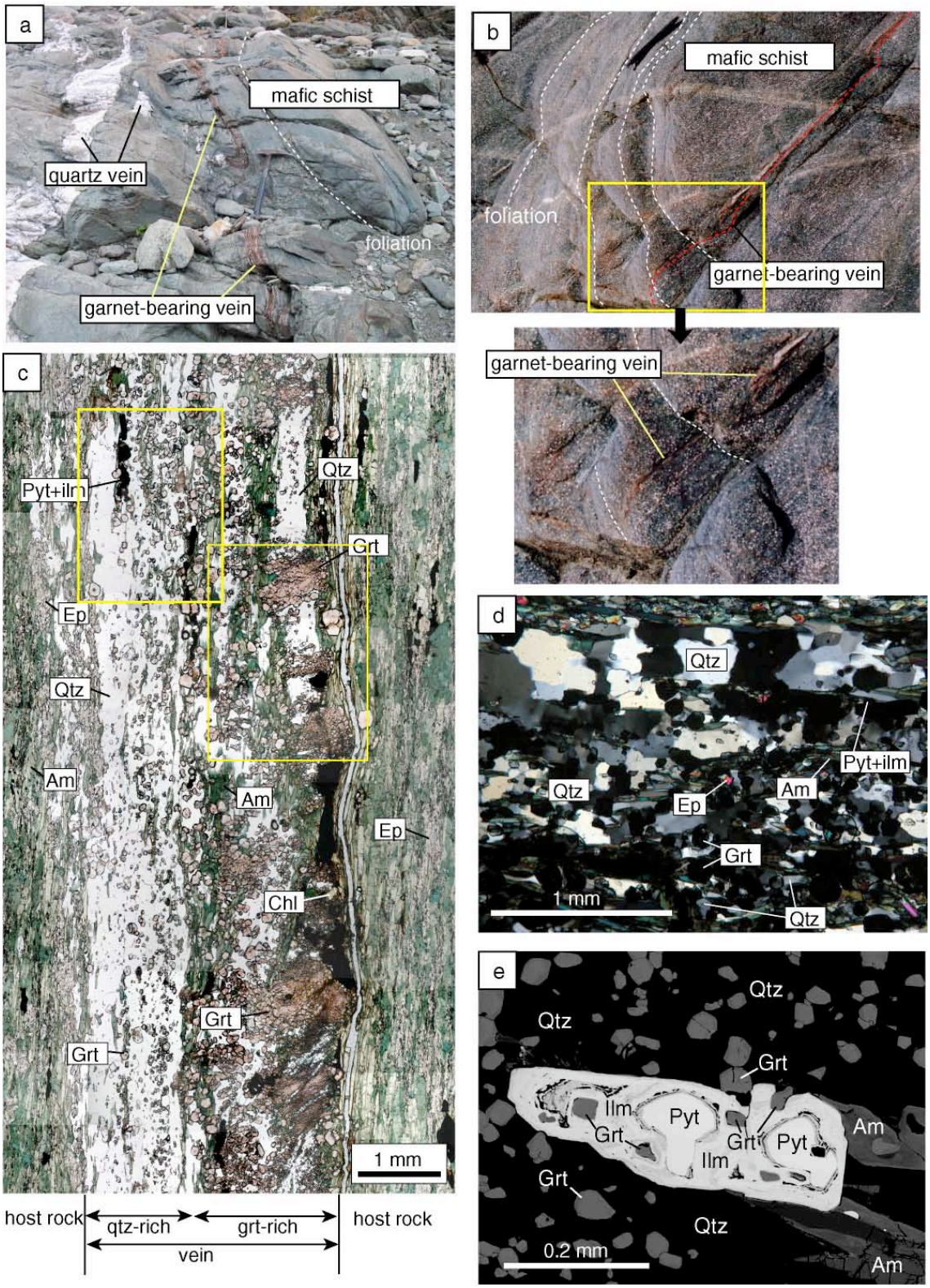
a
mafic schist
quartz vein
foliation
garnet-bearing vein
b
mafic schist
foliation
garnet-bearing vein
garnet-bearing vein
c
Pyt+ilm
Qtz
Grt
Ep
Qtz
Am
Am
Ep
Chl
Grt
Grt
1 mm
host rock
qtz-rich
grt-rich
host rock
vein
d
Qtz
Pyt+ilm
Qtz
Ep
Am
Grt
1 mm
Qtz
e
Qtz
Qtz
Grt
Ilm
Pyt
Grt
Grt
Pyt
Am
Ilm
Grt
Qtz
0.2 mm
Am

Fig. 3

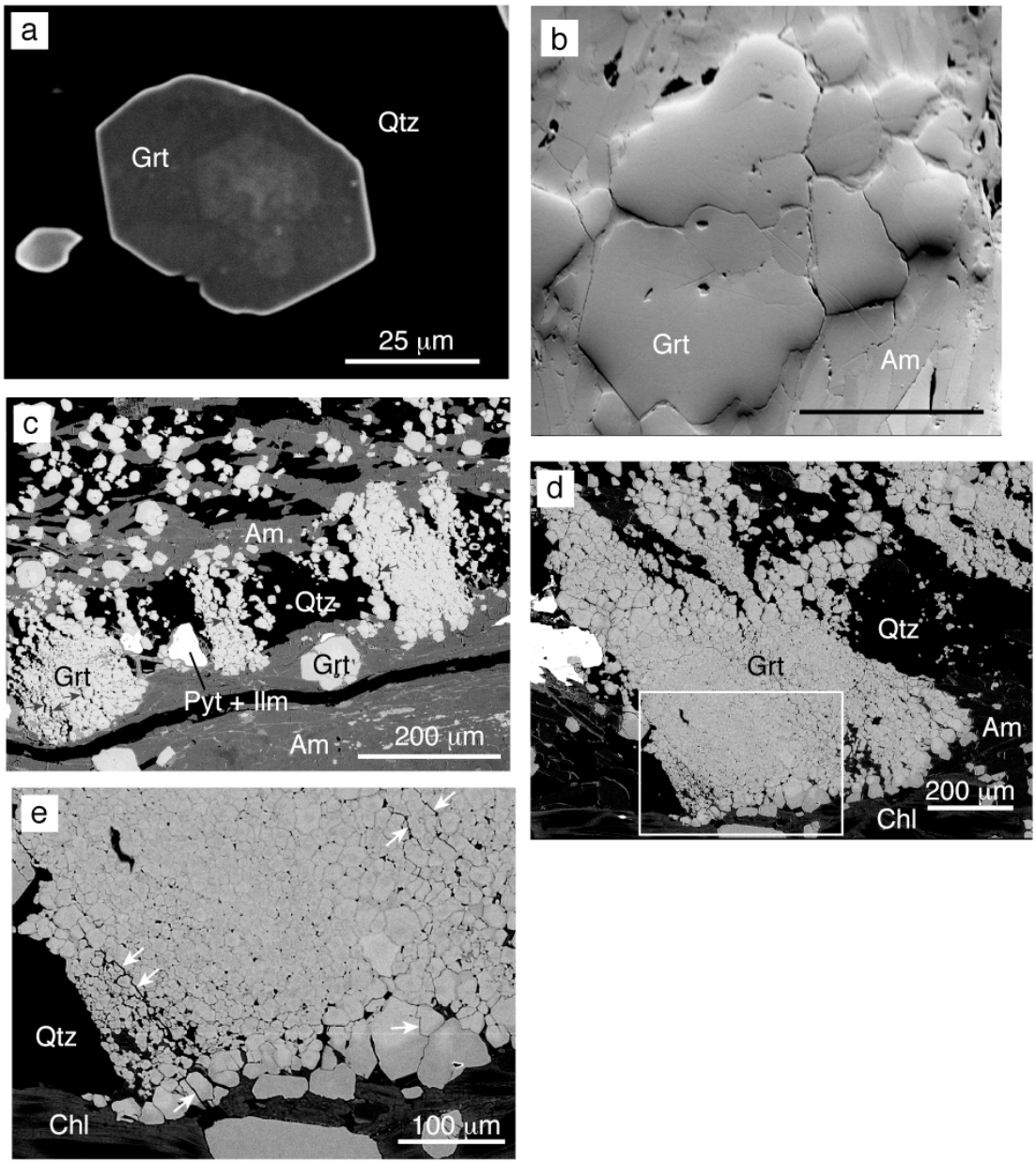
a
Grt
Qtz
25 μm
b
Grt
Am
c
Am
Qtz
Grt
Grt
Pyt + Ilm
Am
200 μm
d
Qtz
Grt
Am
200 μm
Chl
e
Qtz
Chl
100 μm

Fig. 4

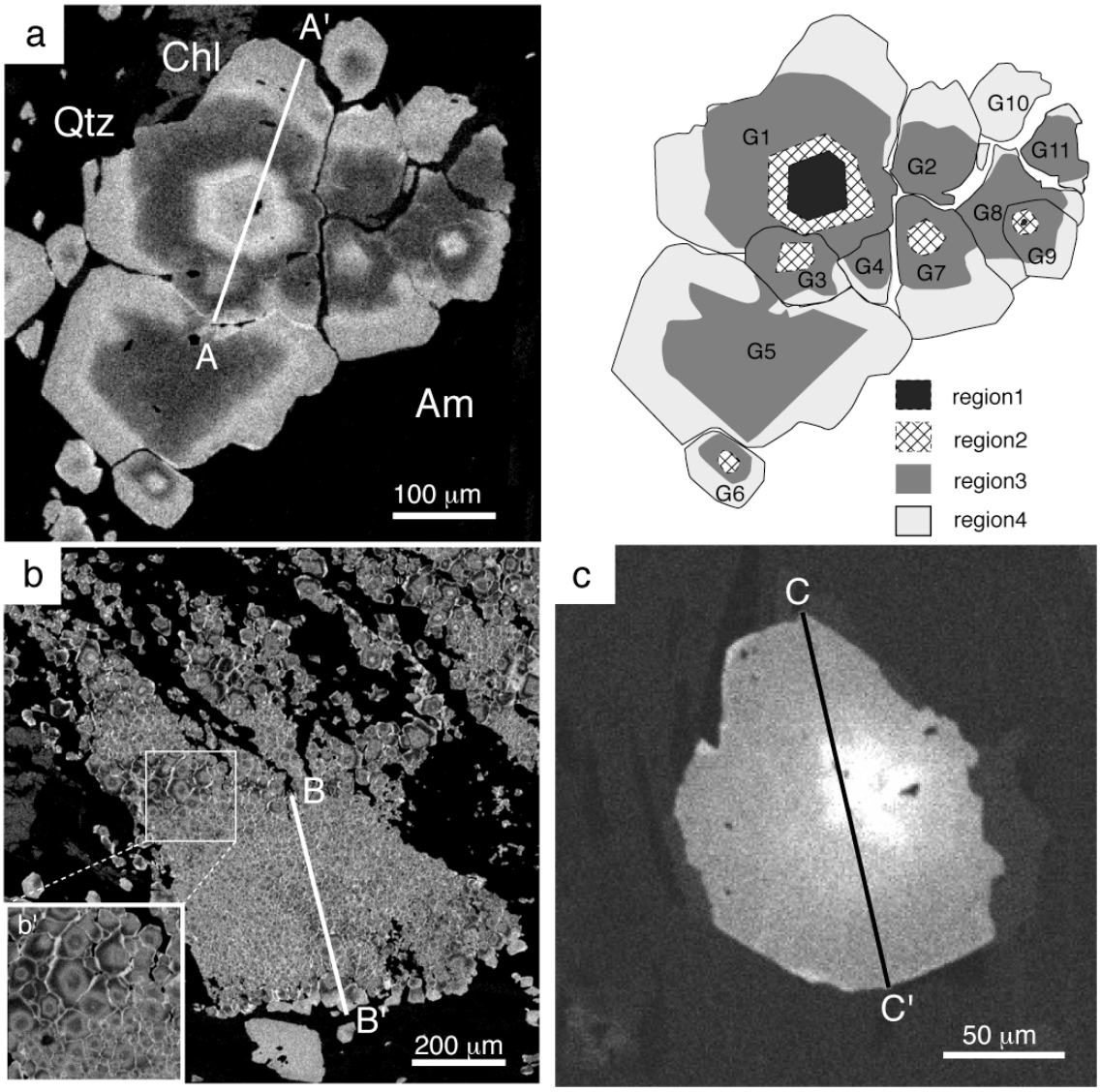
a
Chl
Qtz
A'
A
Am
100 μm
G1
G2
G10
G11
G8
G9
G3
G4
G7
G5
G6
region1
region2
region3
region4
b
B
B'
b'
200 μm
c
C
C'
50 μm

Fig. 5

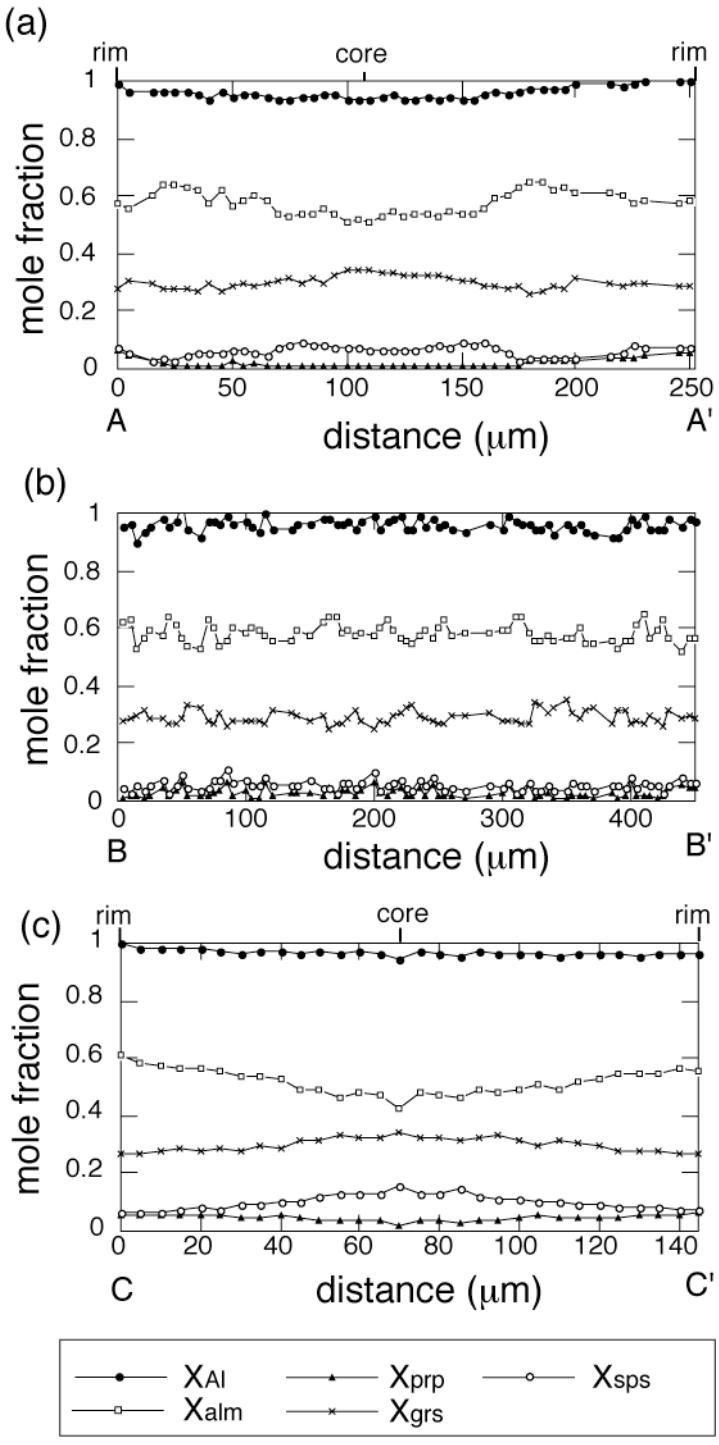
(a)
rim
core
rim
mole fraction
1
0.8
0.6
0.4
0.2
0
0
50
100
150
200
250
A
distance (μm)
A'
(b)
mole fraction
1
0.8
0.6
0.4
0.2
0
0
100
200
300
400
B
distance (μm)
B'
(c)
rim
core
rim
mole fraction
1
0.8
0.6
0.4
0.2
0
0
20
40
60
80
100
120
140
C
distance (μm)
C'
XAl
Xprp
Xsps
Xalm
Xgrs

Fig. 6

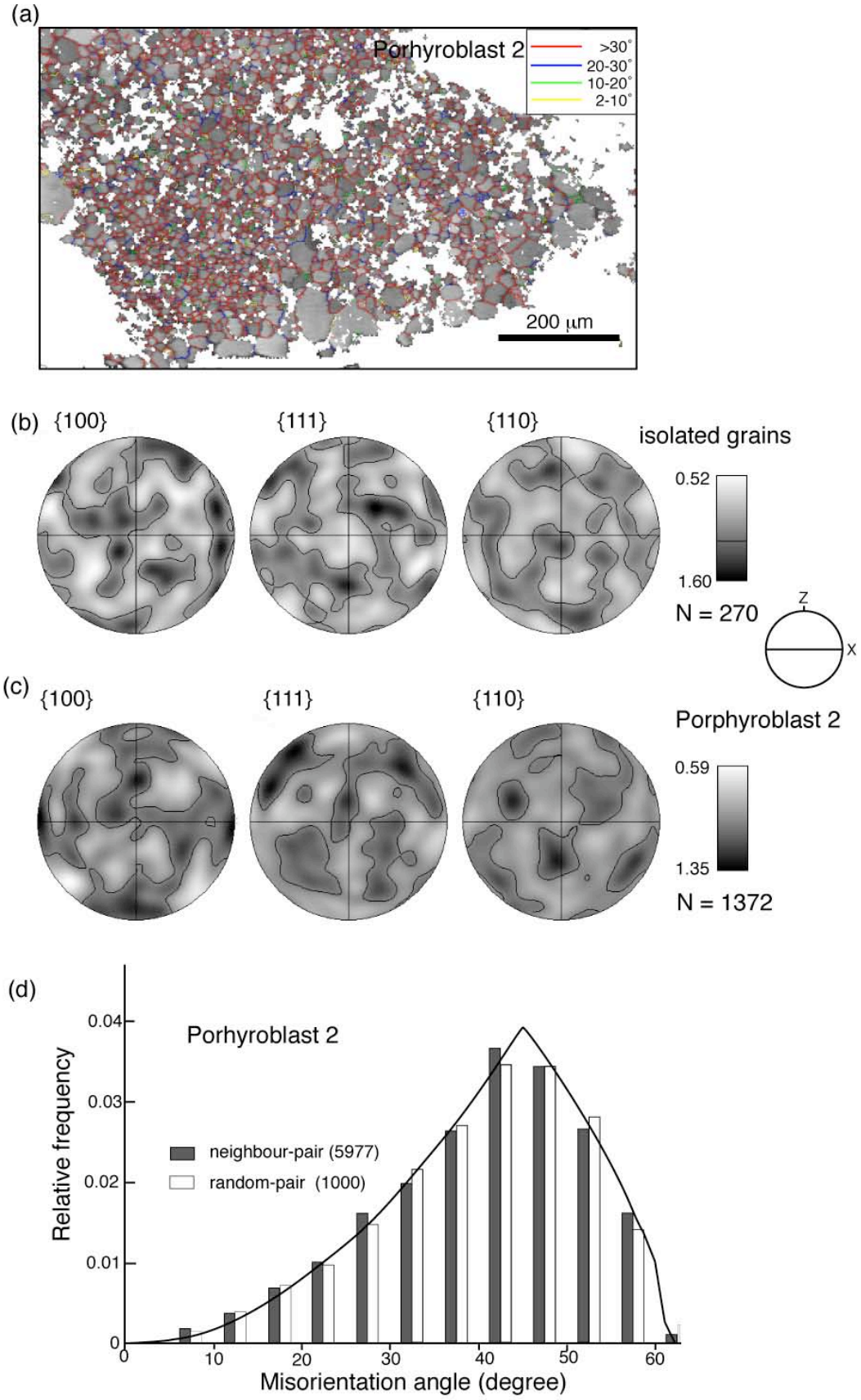
(a)
Porhyroblast 2
>30°
20-30°
10-20°
2-10°
200 μm
(b)
{100}
{111}
{110}
isolated grains
0.52
1.60
N = 270
Z
X
(c)
{100}
{111}
{110}
Porphyroblast 2
0.59
1.35
N = 1372
(d)
Porhyroblast 2
neighbour-pair (5977)
random-pair (1000)
Relative frequency
0.04
0.03
0.02
0.01
0
0
10
20
30
40
50
60
Misorientation angle (degree)

Fig. 7

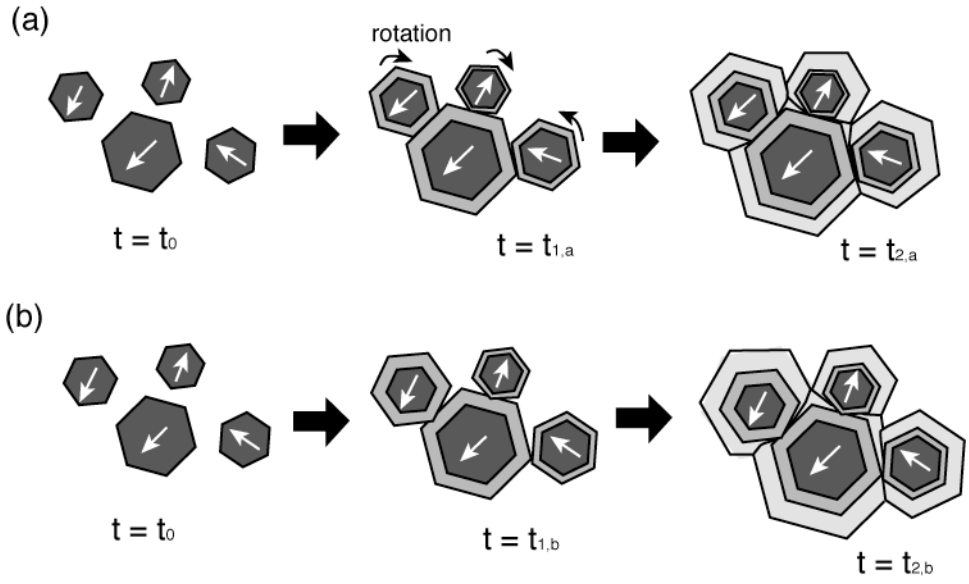

Fig. 8

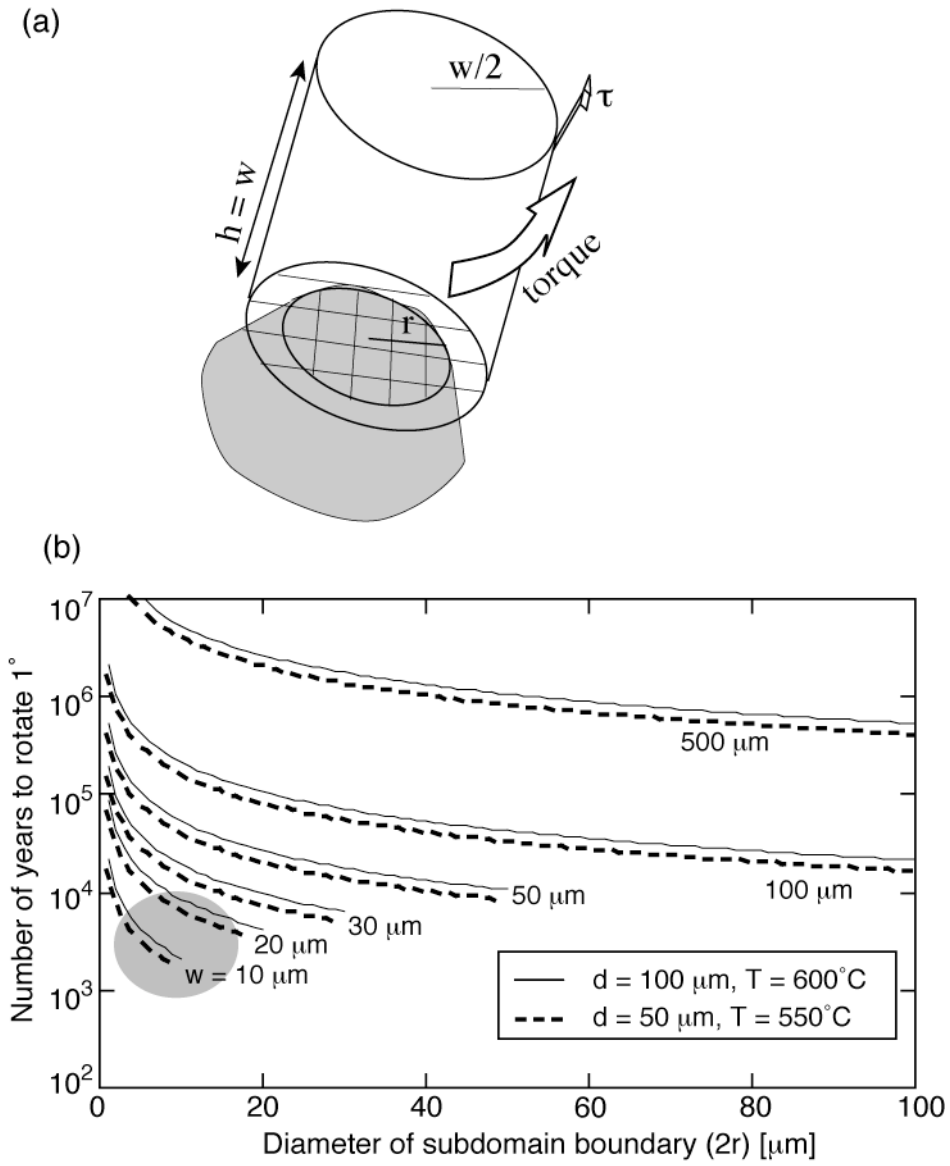
(a)
w/2
τ
h = w
torque
r
(b)
Number of years to rotate 1°
10^7
10^6
10^5
10^4
10^3
10^2
0
20
40
60
80
100
Diameter of subdomain boundary (2r) [μm]
500 μm
100 μm
50 μm
30 μm
20 μm
w = 10 μm
d = 100 μm, T = 600°C
d = 50 μm, T = 550°C